ELSEVIER

Earth and Planetary Science Letters 202 (2002) 709–724

EPSL

www.elsevier.com/locate/epsl

Genetic significance of the trace element content in metamorphic and hydrothermal quartz: a reconnaissance study

T. Monecke *, U. Kempe, J. Götze

Freiberg University of Mining and Technology, Institute of Mineralogy, Brennhausgasse 14, D-09596 Freiberg, Germany

Received 31 May 2002; received in revised form 24 June 2002; accepted 25 June 2002

Abstract

A reconnaissance study on trace elements in metamorphic and hydrothermal quartz was carried out using quartz samples from the tin district Erzgebirge, Germany, the gold mineralization at Kašperské Hory, Czech Republic, and the gold-quartz vein deposits Muruntau and Myutenbai, Uzbekistan. A new method of sample preparation has been developed to prepare pure quartz samples by combining conventional hand-picking with microscopic and spectroscopic studies as well as acid wash/etch procedures. Preparation of monomineralic samples was followed by sample dissolution and measurement by ICP-MS. The metamorphic quartz has very low concentrations of Li ($\leq$0.4 ppm), Al ($\leq$30 ppm), K ($\leq$35 ppm), Rb ($\leq$50 ppb), Sr ($\leq$0.3 ppm), and Y ($\leq$15 ppb). Moreover, it is characterized by light rare earth element enriched lanthanide distribution patterns lacking Eu anomalies. The low element concentrations in metamorphic quartz are interpreted to result from recrystallization. Metamorphic quartz from alteration halos enveloping tin and gold deposits has distinctly different trace element signatures. These differences are related to the hydrothermal overprint of the pre-existing metamorphic quartz by the mineralizing fluids. Hydrothermally altered metamorphic quartz from tin deposits has elevated concentrations of Li ($\geq$0.9 ppm), Al ($\geq$50 ppm), K ($\geq$45 ppm), Rb ($\geq$250 ppb), and Y ($\geq$40 ppb) whereas altered metamorphic quartz from gold deposits is characterized by elevated concentrations of Sr ($\geq$0.5 ppm). The rare earth element distribution patterns of altered metamorphic quartz show variable enrichments of the heavy rare earth elements and frequently display positive Eu anomalies. Hydrothermal vein quartz from the gold deposits usually has elevated Al ($\geq$50 ppm) and Sr ($\geq$0.6 ppm) contents. The lanthanide distribution patterns exhibit variable enrichments of the heavy rare earth elements and commonly show positive Eu anomalies. The elevated Sr concentrations in the quartz from gold deposits are best explained by Sr release during feldspar alteration in the wall rocks. This mechanism may also account for the relative enrichment of Eu in the mineralizing fluids although other processes may not be unambiguously ruled out.

Keywords: quartz; trace elements; rare earths; hydrothermal alteration; ore-forming fluids; mineral deposits; genesis

* Corresponding author. Tel.: +49-3731-39-3472; Fax: +49-3731-39-2610.
E-mail address: tmonecke@mineral.tu-freiberg.de (T. Monecke).

0012-821X/02/$ – see front matter
PII: S0012-821X(02)00795-1

1. Introduction

Trace element determinations on single mineral grains and monomineralic samples have been extensively used in earth sciences for petrogenetic modeling and have become an important tool in ore deposit studies. Although quartz is widely distributed in several common rock types and occurs in many ore deposits, relatively few attempts have been made to investigate the trace element contents of quartz (e.g., [1–6]). These studies have established that the concentrations of many elements in quartz are very low hampering reliable determination by standard analytical methods. Therefore, it is commonly believed that the efforts undertaken to prepare and analyze pure natural quartz samples are not justified by the geological information that can be gathered from the analytical results.

Wünsch [7] and Heynke et al. [8] have shown that the total amount of trace elements contained in quartz can be used to distinguish between metamorphic quartz and hydrothermal vein quartz occurring within the middle to high grade metamorphic terrain of the Erzgebirge, Germany. Furthermore, the distribution patterns of rare earth elements (REEs) may potentially represent an additional source of information to distinguish quartz of different origin and to constrain the environment of quartz formation because the behavior of REEs in metamorphic and hydrothermal fluids has been studied extensively [9–11]. REE distribution patterns of hydrothermal quartz from gold deposits in the Ural Mountains, Russia, were reported by Novgorodova et al. [12]. These authors described a strong positive correlation between gold and the total REE content. Peucker-Ehrenbrink and Schnier [13] analyzed quartz from a shear zone in Bavaria, Germany, and concluded that positive Eu anomalies were indicative of intense feldspar alteration of the wall rocks whereas negative Ce anomalies were related to the oxidizing environment of quartz formation. Vinokurov et al. [14] demonstrated that the REE patterns of hydrothermal quartz from epithermal gold deposits commonly show positive Eu anomalies and slopes that differ from the host rocks whereas the lanthanide distributions of barren samples were found to resemble the wall rock signatures.

Apart from these earlier studies, little systematic work has been done on the geochemical characteristics of metamorphic and hydrothermal quartz and, in particular, on the REE distribution patterns of quartz of different origin. Therefore, the objectives of the present reconnaissance study were: (1) to develop a procedure of sample preparation and low level analysis of metamorphic and hydrothermal quartz yielding reliable trace element data including the REEs at moderate analytical efforts, (2) to obtain data constraining the trace element signatures of metamorphic and hydrothermal quartz, (3) to test whether hydrothermal alteration affects the trace element content of pre-existing metamorphic quartz located within alteration halos of ore deposits, and (4) to demonstrate that information on the nature of mineralizing hydrothermal fluids can be obtained from the study of quartz.

The developed procedure of sample preparation combines conventional hand-picking of pure quartz with microscopic investigations (optical microscopy, cathodoluminescence (CL), and scanning electron microscopy (SEM)), acid wash/etch procedures, and spectroscopic tests to confirm the purity of the samples (photoluminescence, infrared stimulated optical luminescence (IRSL), and infrared spectroscopy). Low level trace element analysis was carried out by inductively coupled plasma mass spectrometry (ICP-MS). The metamorphic and hydrothermal samples analyzed were collected from three well-characterized localities, namely from the tin mining district Erzgebirge, Germany, the gold-quartz vein deposit Kašperské Hory, Czech Republic, and the gold deposits of Muruntau and Myutenbai, Uzbekistan.

2. Sample selection

In order to test for variations in the trace element signatures of metamorphic and hydrothermal quartz, samples were collected from metamorphic quartz bodies located at different distances (up to several hundred meters) from tin–tungsten and gold deposits. Moreover, hydro-

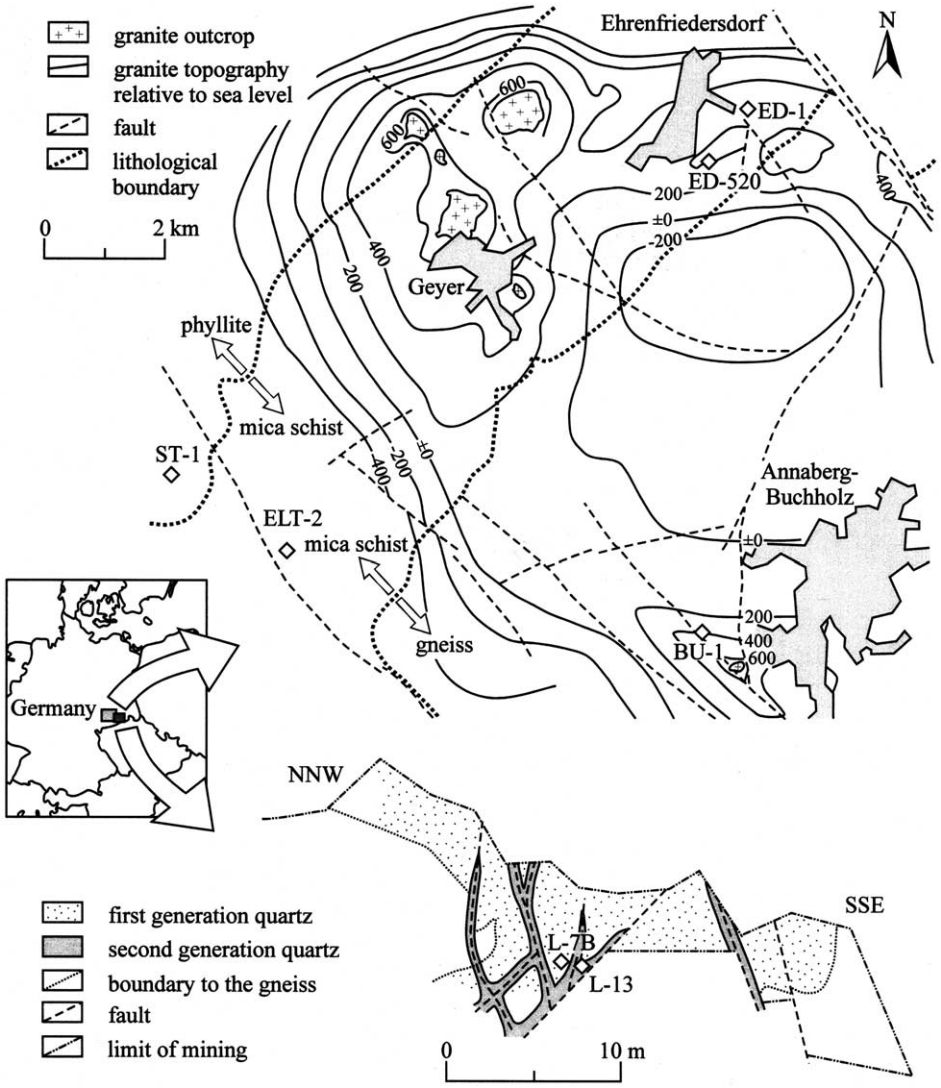

Fig. 1. Geological map of the Middle Erzgebirge, Germany, showing the topography of the Li–F granites [15] and simplified map of the Lauenstein vein-like quartz body in the Eastern Erzgebirge, Germany (Linnemann, personal communication). The figure displays the sample locations.

thermal vein quartz from the two gold deposits was sampled to allow comparison of the trace element signatures of hydrothermal quartz from deposits of different geological settings.

In analogy to the studies by Wünsch [7] and Heynke et al. [8], several samples were taken for analysis from quartz bodies occurring in metamorphic rocks of the Middle and Eastern Erzgebirge, Germany (Fig. 1). In the Middle Erzgebirge, the quartz-hosting metamorphic rocks are phyllite, mica schist, as well as para- and orthogneiss. The metamorphic rocks are intruded by Hercynian Li–F granites that form a horseshoe-shaped intrusive complex. Cassiterite mineralization occurs in greisen bodies within the endocontact and in vein zones within the exocontact of the granites [15,16]. Two samples were taken distal to the granite intrusions from quartz lenses located in unaltered phyllite (sample ST-1) and garnet-bearing mica schist (sample ELT-2). Hydrother-

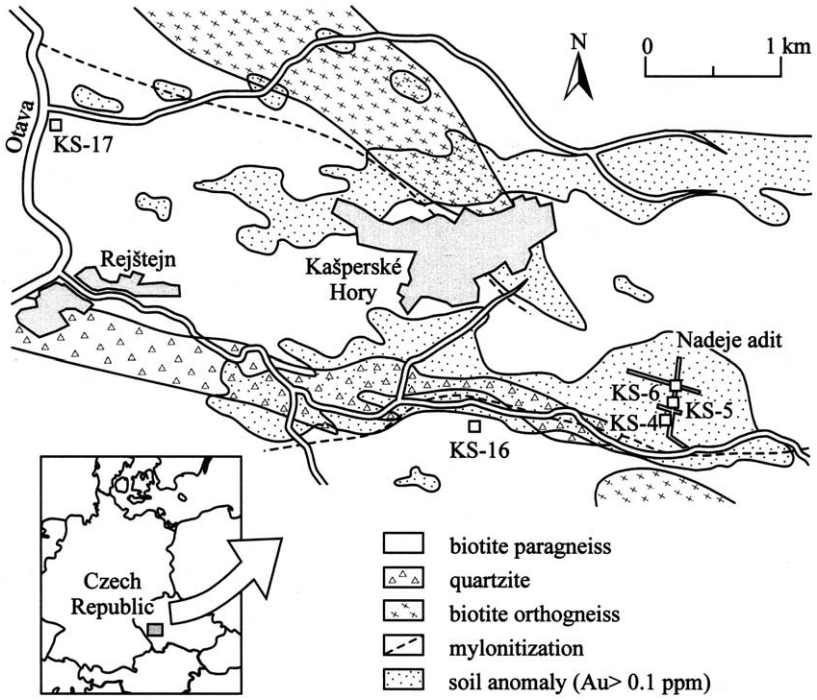

Fig. 2. Geological map of the Kašperské Hory gold deposit, Czech Republic, with soil geochemical anomalies and the locations of the sampled quartz bodies [17].

mal mineralization is not known from this area. In the area of tin mineralization located to the east, one quartz was sampled distal to the Ehrenfriedersdorf tin deposit from unaltered garnet-bearing mica schist located northerly to a granite cupola at a distance of 300 m to the steeply sloping granite surface (sample ED-1). An additional sample originates from a quartz lens in altered tourmaline-bearing paragneiss located 300 m above a granite cupola close to ancient tin mining (sample BU-2). Finally, one quartz lens was taken from altered garnet- and tourmaline-bearing mica schist in the underground mine of Ehrenfriedersdorf at a distance of 28 m from the granite (sample ED-520). The last two samples were collected to test whether hydrothermal alteration related to tin mineralization affects the trace element signature of pre-existing metamorphic quartz.

Two quartz samples were taken from a 2 m thick and 40 m long NNW–SSE striking vein-like quartz body that is arranged into the schistosity of anatectic gneiss at Lauenstein in the Eastern Erzgebirge (Fig. 1). From the geological evidence and fluid inclusion studies, the quartz body of Lauenstein has been previously regarded to be a 'prototype' of quartz that formed as a mobilization product of high grade metamorphism [8]. Most of the vein-like quartz body is composed of first generation white to gray massive quartz (sample L-7B) that is frequently cut by faults that gave rise to the formation of second generation gray massive quartz. The latter quartz frequently contains transparent crystals (sample L-13).

Metamorphic quartz lenses were also collected from the Kašperské Hory gold district, Czech Republic. The low sulfide gold mineralization is hosted by paragneiss and migmatite with intercalated quartzite, calc-silicate rocks, felsic volcanic rocks, amphibolite, and marble [17]. The mineralization occurs in E–W trending zones containing native gold of high fineness (>910), Au–Bi–Te minerals, and scheelite [17–19]. The sampling strategy applied at Kašperské Hory was similar

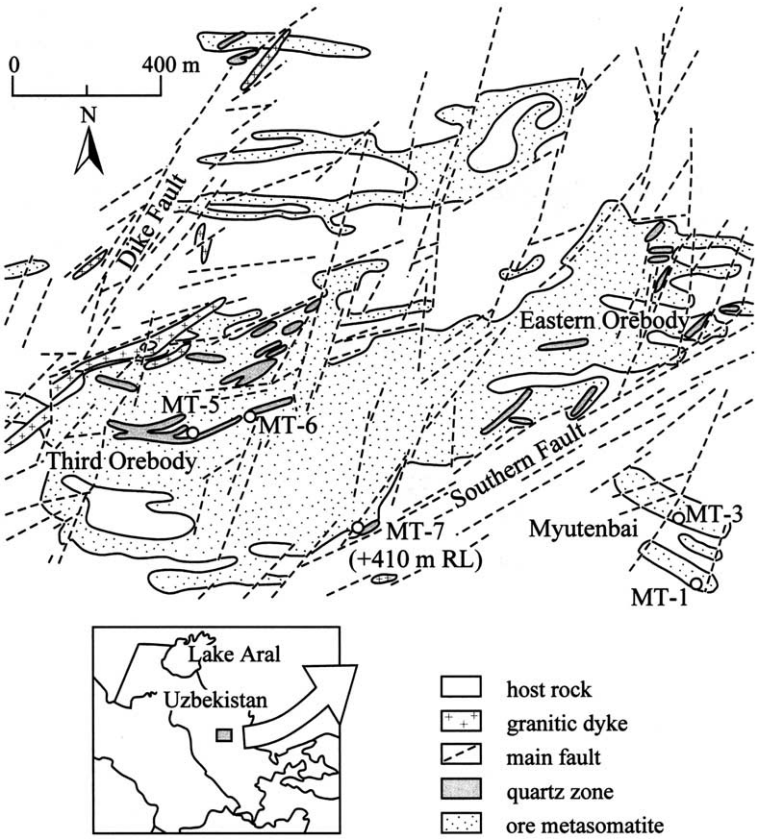

Fig. 3. Geological map of the +78 level of the Muruntau and Myutenbai gold deposits, Uzbekistan, showing the sample locations [33].

to that used in the tin district of the Middle Erzgebirge, i.e., the samples were taken at different distances from the gold mineralization (Fig. 2). One quartz was collected distal to the Kašperské Hory deposit from a metamorphic lens arranged into the shallow N dipping and E–W trending foliation of the biotite paragneiss (sample KS-17). A second quartz was collected from a quartz lens in a similar structural position, but located closer to the gold mineralization (sample KS-16). One sample was taken from a metamorphic quartz lens in the underground Nadeje adit where gold mineralization occurs (sample KS-6). This quartz contains numerous steeply dipping secondary fluid inclusion trails causing visible dark striations. Two additional samples were taken from the Nadeje adit representing examples of gold-bearing quartz veins that developed along steeply N dipping and E–W trending shear planes (samples KS-4 and KS-5).

Samples of metamorphic quartz and hydrothermal vein quartz from the gold mines of Muruntau and Myutenbai situated in the Central Kyzylkum Desert, Uzbekistan, were included in the present study for comparison to quartz from Kašperské Hory. At Muruntau and Myutenbai, gold occurs in intensely altered wall rocks (greenschist to amphibolite facies metamorphosed siltstone and shale with interbedded sandstone) as well as in quartz veins. Two types of veins can be distinguished: (1) 'flat' (subparallel to the foliation) millimeter to several centimeters wide veins that are frequently boudinaged or folded and (2) steeply dipping centimeter to meter wide 'central' veins that are associated with steeply dipping micrometer to centimeter wide 'stockwork' veins with

no continuity on the meter scale in any direction [20–22]. The mineralized zones of Muruntau and Myutenbai are separated by the 'Southern Fault' (Fig. 3). The presence of a granite body below the Myutenbai deposit has been documented by deep drilling [21,22]. At Muruntau, one sample was collected from a quartz nodule that was arranged into the foliation of the altered wall rocks (sample MT-6). The altered wall rocks contained native gold together with secondary microcline. The quartz nodule was located adjacent to a 'central' vein that was also sampled (quartz MT-5). One sample was taken from a similar quartz vein at a higher mining level and adjacent to the 'Southern Fault' (sample MT-7). At Myutenbai, two samples were collected from steeply dipping quartz veins. One sample originated from a 1.5 m thick 'central' quartz vein (sample MT-1) whereas the other sample was taken from a 1 cm thick 'stockwork' veinlet (quartz MT-3).

3. Analytical procedure

The preparation of monomineralic samples was preceded by optical microscopy, CL microscopy, and SEM on thin sections. These studies were primarily carried out to test whether pure quartz could be obtained by hand-picking and to constrain the textural relationships between quartz and other minerals. The microscopic studies also provided information on the quartz texture and luminescence behavior essential for the interpretation of the trace element data (see below). The CL examinations were carried out using a 'hot cathode' microscope HC1-LM operated at 14 kV with a current density of $\sim$10 μA/mm^2 [23]. The SEM investigations were performed on a JEOL 6400 equipped with a Noran EDX detector Series II operated at 20 kV and 600 pA. The CL technique proved to be particularly useful to identify minute amounts of apatite (yellowish or greenish CL), calcite (orange CL), feldspar (greenish or bluish CL), and scheelite (bluish or yellowish CL) contained in the quartz matrix. The microscopic investigations revealed that the specimens contained relatively large zones of quartz lacking mineral inclusions that could be easily sampled by hand-picking. With the exception of calcite in the samples from Muruntau and Myutenbai, most of the minerals could be easily identified and removed from the samples (Table 1).

The thin section investigations were followed by the preparation of high purity samples and tests to confirm the purity of the material. Initially, the samples were crushed and sub-samples (150–300 mg) of pure quartz grains without visible impurities were hand-picked using a binocular microscope. The choice of the sample grain size, which was in general not larger than 200 μm, was controlled by several factors, which included the transparency and the mineralogical purity. All samples containing calcite and/or scheelite (Table 1) were hand-picked a second time under ultraviolet light (254 nm). The pure quartz was stored in acid cleaned glass tubes.

A fraction of each sample was investigated by IRSL to detect feldspar impurities (other IRSL-active minerals were not present). Even tiny feldspar grains or inclusions can be detected in the IRSL non-active quartz matrix. The samples were exposed to β-radiation (1.28 Gy/min) for 3000 s. The IRSL was measured 10 h after irradiation using the TL/OSL system TL-DA-12 (Risø National Laboratory, Denmark) operated at 8 mW/cm^2 with the optical filter BG 39 (Schott). Sample ED-520 showed a higher counting rate than a pure synthetic quartz (Merck) that was used as a reference material. Since surfaces of feldspar grains appear dull after 20 s HF etching, the feldspar impurities could be readily identified and removed from the sample after treatment. A repeated IRSL measurement of the sample did not yield elevated counting rates.

Thereafter, all samples were repeatedly washed with diluted HNO_3 and ultrapure water. The samples were crushed to a grain size of approximately 30 μm using a carefully pre-cleaned agate mortar and pestle. Tests on the mortar and the pestle showed that contamination introduced in this way could be neglected. A fraction of each powdered sample was investigated by Fourier-transform infrared spectroscopy (FT-IR) with a Nicolet 510 FT-IR to search for further impurities. Calcite was detected in samples MT-1, MT-3, and MT-6 by this method. According to the mi-

croscopic investigations, traces of calcite were also present in samples MT-5 and MT-7. Therefore, all powdered samples from Muruntau and Myutenbai were treated with concentrated HNO_3 to dissolve calcite. Repeated FT-IR measurements on the acid-cleaned samples did not reveal the presence of further impurities.

The powdered samples (100 mg) were digested in glassy carbon vessels with 5 ml concentrated HF and 3 ml concentrated HNO_3 at 50°C (30 min) and subsequently evaporated to dryness at 100°C. The evaporation procedure was then repeated. After cooling of the vessels, the residues were picked up with 2 ml HNO_3 and transferred to disposable polypropylene tubes. 4 ml ultrapure water was utilized for rinsing the vessels. This solution was also transferred to the polypropylene tubes along with 2 ml ultrapure water used for

Table 1
Description of the samples investigated

Sample	Quartz microtexture	Cathodoluminescence	Mineral association
Tin mining district Middle and Eastern Erzgebirge, Germany			
ST-1	xnm, undulose ext, equigranular, irregular gb	stable brown, faint unstable yellow on gb	ap, chl, ms, sl
ELT-2	xnm, undulose ext, irregular gb	stable brown, faint unstable greenish on gb	ms
ED-1	xnm, undulose ext, irregular gb	stable brown	bt, ms
ED-520	xnm to hpm, rare undulose ext, polycrystalline, irregular to regular gb	intense unstable dark green, stable brown	bt, fs, ms
BU-2	xnm to hpm, polycrystalline, irregular gb	stable bluish-black	bt, ms
L-7B	xnm, undulose ext, deformation lamellae, subgrains, transecting bands of small recrystallized grains	intense unstable greenish blue, stable brown	bt, chl, fs, ms, rt
L-13	idm to hpm, slight undulose ext, relatively regular gb	unstable blue, stable brown	bt, hem, mnz, ms, zrn
Gold deposit Kašperské Hory, Czech Republic			
KS-4	large porphyroclasts, undulose ext, irregular gb, matrix of small recrystallized grains	intense unstable yellowish green, stable brown	au (22 g/t), bi, bis, chl, hd, mo, ms, py
KS-5	large xnm grains, undulose ext, irregular gb, areas of small recrystallized grains	unstable blue, stable brown	bt, cal, chl, sl
KS-6	large porphyroclasts, undulose ext, irregular gb, matrix of small recrystallized grains	intense unstable yellowish green, stable brown	ms
KS-16	xnm, elongate subgrains, undulose ext, irregular gb	stable bluish-black	ap, cal, bt, mnz, zrn
KS-17	xnm, elongate subgrains, undulose ext, irregular gb, areas of small recrystallized grains	stable bluish-black	ap, bt, ilm
Gold deposits Muruntau and Myutenbai, Uzbekistan			
MT-1	xnm, undulose ext, irregular gb	stable bluish-black	cal, ccp, hem, py, sl
MT-3	xnm, undulose ext, irregular gb, areas of strong recrystallization	stable bluish-black	ap, au, cal, ccp, chl, pl, py, sl
MT-5	xnm, undulose ext, irregular gb	stable bluish-black	ap, cal, chl, fs, sl
MT-6	xnm, undulose ext, irregular gb	stable bluish-black	cal, chl
MT-7	xnm, deformation lamellae, subgrains, bands of small recrystallized grains	stable bluish-black	cal, sl

Microtexture: ext = extinction, gb = grain boundaries, hpm = hypidiomorphic, idm = idiomorphic, xnm = xenomorphic. Minerals: ap = apatite, au = native gold, bi = native bismuth, bis = bismuthinite, bt = biotite, cal = calcite, ccp = chalcopyrite, chl = chlorite, fs = feldspar, hd = hedleyite, hem = hematite, ilm = ilmenite, mnz = monazite, mo = molybdenite, ms = muscovite, pl = pilsenite, py = pyrite, rt = rutile, sl = scheelite, zrn = zircon.

Table 2
Trace element concentrations of the investigated quartz samples

	ST-1	ELT-2	ED-1	ED-520	BU-2	L-7B	L-13	KS-4	KS-5	KS-6	KS-16	KS-17	MT-1	MT-3	MT-5	MT-6	MT-7
Concentration in ppm																	
Li	0.33	0.16	0.40	0.90	1.06	5.69	130	0.96	0.04	0.97	1.97	0.83	0.43	0.47	0.22	0.41	0.06
Na	61.9	67.2	33.1	41.0	28.4	75.3	54.7	75.6	56.3	54.6	24.8	14.7	74.8	64.3	27.7	51.2	41.8
Mg	41.0	7.0	8.4	9.4	18.6	9.2	3.7	16.3	10.8	9.6	147	4.47	30.1	63.9	7.7	9.6	5.6
Al	29.1	28.6	14.5	121	53.7	120	611	147	130	101	93.0	87.1	71.4	76.9	24.3	23.2	47.4
K	19.1	15.2	35.5	55.3	46.8	82.3	25.4	64.1	14.6	53.2	52.7	7.89	23.6	19.9	10.9	12.6	18.6
Ca	20.0	16.0	10.5	125	16.7	30.0	282	43.6	107	48.3	18.0	8.85	77.2	22.1	9.5	19.5	99.7
Mn	0.32	0.13	0.39	0.51	0.60	0.55	1.85	0.48	0.53	0.57	0.59	0.21	3.94	1.45	0.25	0.30	1.96
Sr	0.30	0.28	0.22	0.19	0.15	0.83	0.96	0.65	0.61	0.71	0.52	0.16	1.12	0.91	0.64	0.61	1.20
Ba	12.8	11.9	0.23	2.93	2.07	11.0	0.92	9.47	1.24	5.20	3.29	2.30	2.23	3.68	1.38	4.63	0.81
Concentration in ppb																	
Co	20	70	70	50	30	10	30	20	10	30	422	41	20	20	10	20	7
Rb	50	30	50	290	250	500	70	220	50	140	285	34	120	90	20	40	95
Y	10.6	15.4	13.2	108	40.3	12.5	38.9	15.2	32.3	16.9	7.1	6.4	122	15.6	6.1	15.3	5.6
La	44.3	25.7	22.5	30.7	47.6	21.1	65.4	16.3	23.0	11.2	7.9	16.0	129	54.3	24.5	33.7	16.0
Ce	81.2	123	383	110	94.3	46.7	107	45.4	44.2[a]	49.7	30.0[a]	49.6[a]	263	111	39.0	84.3	37.4[a]
Pr	5.0	3.6	4.3	4.8	10.9	3.3	8.5	1.6	4.3	2.5	1.6	2.3	31.9	9.2	2.7	5.7	3.5
Nd	17.8	12.6	15.9	19.2	37.5	12.3	30.9	4.4	17.6	9.4	6.7	7.7	125	29.3	10.2	17.5	12.5
Sm	3.4	3.0	3.1	5.4	6.4	2.2	5.6	0.9	4.1	2.2	2.0	1.3	32.2	4.5	1.9	2.9	2.1
Eu	1.4	1.1	0.9	5.4	1.4	1.4	1.6	1.6	1.8	1.4	0.6	0.4	39.5	4.3	0.6	0.9	1.4
Gd	3.9	2.8	3.3	9.1	5.4	2.5	5.9	1.3	4.2	2.7	2.2	0.9	39.7	5.2	1.3	2.8	1.6
Tb	0.6	0.4	0.5	2.2	0.8	0.4	0.9	0.2	0.7	0.5	0.3	< 0.2	6.1	0.6	0.2	0.5	0.2
Dy	2.6	2.0	2.9	15.2	3.8	2.5	5.5	1.6	5.5	3.4	1.7	0.9	34.5	3.5	1.0	3.1	0.9
Ho	0.6	0.3	0.6	3.7	0.7	0.6	1.1	0.4	1.2	0.8	0.3	< 0.2	6.1	0.7	0.2	0.7	0.2
Er	1.4	0.8	1.6	12.3	1.8	1.6	3.2	1.1	3.5	2.5	0.9	0.6	14.6	2.1	0.5	2.1	0.5
Tm	0.2	< 0.2	0.2	1.8	0.2	0.2	0.5	0.2	0.5	0.4	< 0.2	< 0.2	1.6	0.3	< 0.2	0.3	< 0.2
Yb	1.0	0.5	1.3	11	1.3	1.2	3.0	1.2	3.3	2.4	0.9	0.5	7.1	1.5	0.4	1.9	0.5
Lu	< 0.2	< 0.2	< 0.2	1.7	0.2	< 0.2	0.5	< 0.2	0.5	< 0.2	< 0.2	< 0.2	0.8	0.2	< 0.2	< 0.2	< 0.2
Th	< 2	< 2	< 2	< 2	< 2	< 2	< 2	< 2	< 2	< 2	< 2	3	< 2	< 2	< 2	< 2	3
U	< 2	< 2	< 2	< 2	< 2	< 2	13	< 2	25	< 2	7	4	11	12	< 2	< 2	2
Chondrite normalized interelemental ratios																	
La_n/Yb_n	30.7	35.6	12.0	1.9	25.4	12.2	15.1	9.4	4.8	3.2	6.1	22.2	12.6	25.1	42.4	12.3	22.2
La_n/Sm_n	8.2	5.4	4.5	3.6	4.7	6.0	7.3	11.4	3.5	3.2	2.5	7.7	2.5	7.6	8.1	7.3	4.8
Gd_n/Yb_n	3.2	4.6	2.1	0.7	3.4	1.7	1.6	0.9	1.1	0.9	2.0	1.5	4.6	2.9	2.7	1.2	2.6
Ce/Ce*	1.3	3.1	9.3	2.2	1.0	1.3	1.1	2.1	1.1	2.3	2.0	2.0	1.0	1.2	1.1	1.5	1.2
Eu/Eu*	1.2	1.2	0.9	2.3	0.7	1.8	0.8	4.5	1.3	1.7	0.9	1.1	3.4	2.7	1.2	1.0	2.3

The anomalies are defined as $Ce/Ce^* = Ce_n/\sqrt{La_n \cdot Pr_n}$ and $Eu/Eu^* = Eu_n/\sqrt{Sm_n \cdot Gd_n}$.

[a] Due to initial analytical problems the Ce concentration in the sample had to be determined independently from the other lanthanides in a second run.

further rinsing. Rh solution was added as an internal standard for the ICP-MS measurements. The solutions in the tubes were subsequently made up with ultrapure water to a volume of 10 ml [24].

ICP-MS analysis was carried out using a Perkin Elmer Sciex Elan-5000 quadrupole instrument with a cross-flow nebulizer and a rhyton spray chamber. Analytes having low concentrations were directly measured in the undiluted sample solution. To allow measurement of analytes having elevated concentrations, a split of the sample solution was diluted as required and the corresponding amount of Rh solution was added to keep the concentration of the internal standard constant. The application of this scheme allowed measurement of all analytes in samples having variable trace element concentrations. The precision and accuracy of the ICP-MS measurements were evaluated by analysis of the glass sand reference material UNS-SpS. The relative standard deviations for most analytes were below 10%. Additional information on the analytical procedure including total processing blanks and detection limits is presented elsewhere [24].

4. Results

The results of the microscopic investigations are given in Table 1. The trace element data are listed in Table 2 together with chondrite normalized element ratios used to characterize the REE patterns. Chondrite normalization is based on the data given by Anders and Grevesse [25].

The three metamorphic quartz samples collected distal to the tin mineralization in the Middle Erzgebirge (samples ST-1, ELT-2, and ED-1) are characterized by a stable brown CL and show unstable yellow or greenish colors along grain

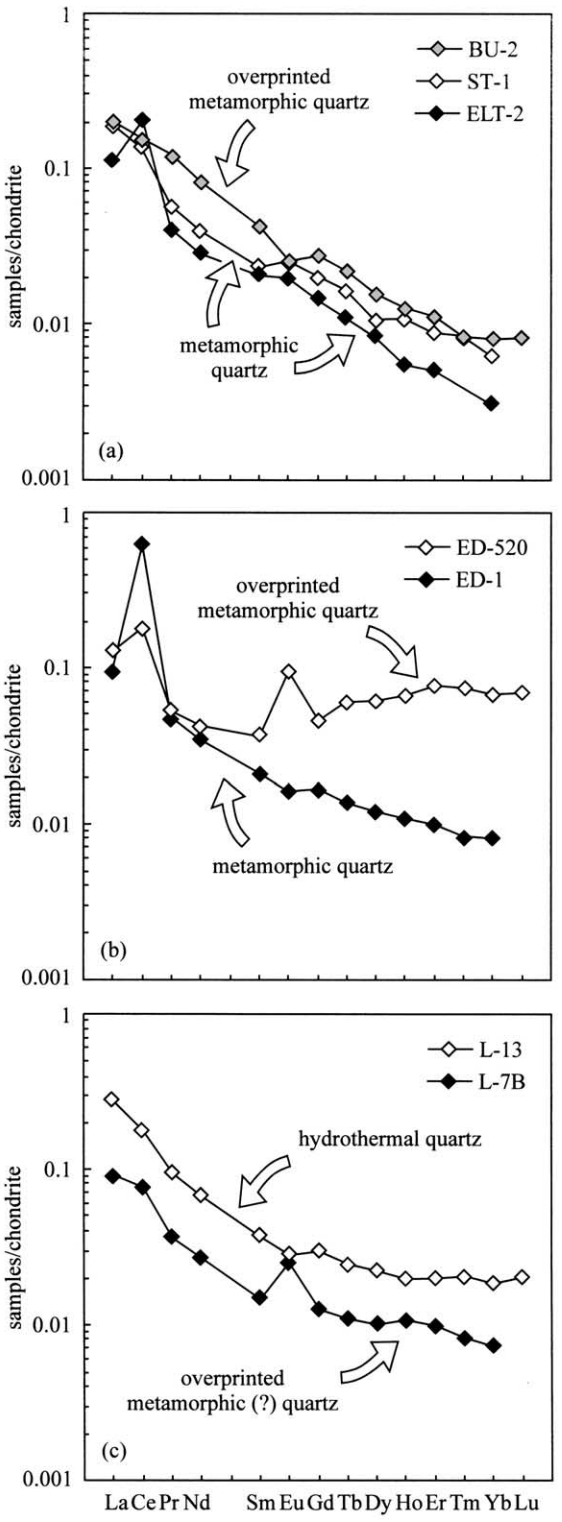

Fig. 4. Chondrite normalized lanthanide distributions of quartz from the tin mining district Erzgebirge, Germany: (a) REE distribution patterns of samples ST-1, ELT-2, and BU-2 from the Middle Erzgebirge, (b) REE distribution patterns of samples ED-1 and ED-520 from the Middle Erzgebirge, and (c) REE distribution patterns of samples L-7B and L-13 from Lauenstein in the Eastern Erzgebirge.

boundaries. An interaction of the metamorphic quartz bodies with hydrothermal fluids related to the deposit formation can be excluded from the field evidence as neither alteration nor hydrothermal veins were evident in the outcrops. Moreover, the microscopic investigations did not reveal evidence for hydrothermal alteration of the quartz. The Al contents in the samples are below 30 ppm and K concentrations range up to 35 ppm. The samples have low Li, Rb, Sr, and Y concentrations and their lanthanide distributions are similar. The normalized REE distribution patterns are enriched in the light rare earth elements ($LREE_n$) and depleted in the heavy rare earth elements ($HREE_n$). Pronounced positive Ce anomalies were observed in two samples (Fig. 4).

The CL behavior of the samples taken from the metamorphic quartz lenses located within the hydrothermal alteration halo enveloping the Li–F granite intrusions (samples ED-520 and BU-2) is distinctly different (Table 1). The metamorphic quartz sampled at a larger distance to the granite shows a stable bluish-black emission whereas the quartz sampled closer to the granite contact is typified by a transient CL with an unstable dark green and a stable brown component. In comparison to metamorphic quartz located outside the alteration halo, the two samples show distinctly higher Li, Al, K, Rb, and Y concentrations. The sample taken from the metamorphic quartz lens located away from the granite is typified by a $LREE_n$ enriched lanthanide distribution pattern that lacks an Eu anomaly. In contrast, the REE distribution pattern of the quartz collected close to the granite is kinked and exhibits a positive Eu anomaly. In comparison to sample ED-1 collected from unaltered garnet-bearing mica schist, the quartz from the altered garnet-bearing mica schist shows a pronounced, but less strong, positive Ce anomaly (Fig. 4).

The quartz samples from Lauenstein represent two different quartz generations. The first generation quartz (sample L-7B) shows an unstable greenish blue and a stable brown CL. The quartz has elevated Li, Al, K, Rb, and Sr concentrations and is characterized by a slightly kinked REE pattern with weak positive Ce and Eu anomalies (Fig. 4). The second generation quartz (sample L-13) shows an unstable blue CL emission and a stable brown CL color. The quartz has the highest Li, Al, Sr, and U concentrations of all investigated samples from the Erzgebirge. However, the K and Rb contents are much lower than those of the first generation quartz. The REE distribution pattern of the second generation quartz is characterized by a decrease of the normalized lan-

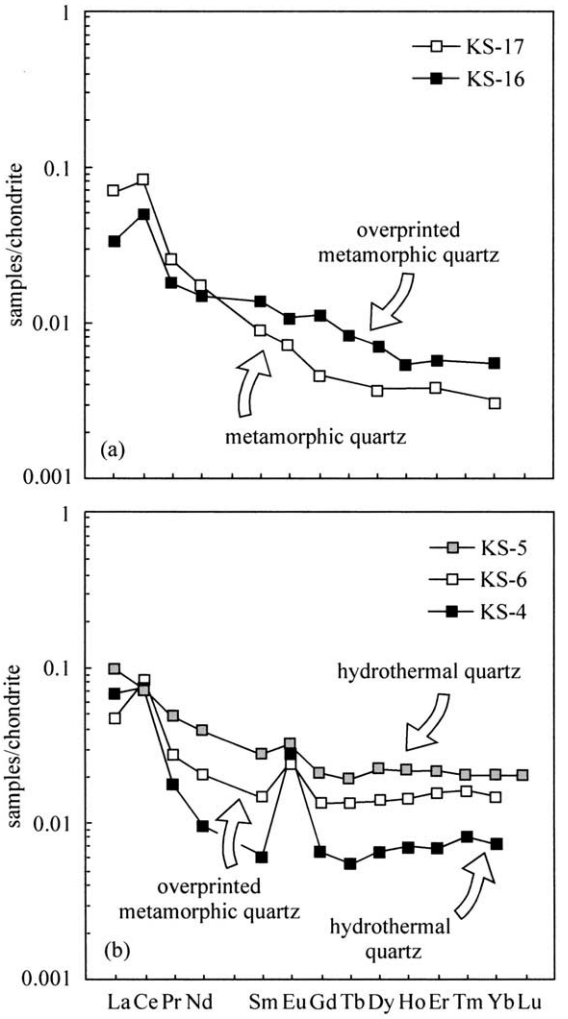

Fig. 5. Chondrite normalized lanthanide distributions of quartz from the Kašperské Hory gold deposit, Czech Republic: (a) REE distribution patterns of samples KS-16 and KS-17 collected from outside the deposit and (b) REE distribution patterns of samples KS-4, KS-5, and KS-6 sampled in the Nadeje adit.

thanide concentrations from La to Sm and has an almost horizontal shape from Gd to Lu (Fig. 4).

The two quartz lenses collected outside the mineralized zones of the Kašperské Hory gold deposit (samples KS-16 and KS-17) were typified by a stable bluish-black CL color. The K and Sr contents are elevated in the metamorphic quartz collected close to the mineralization (KS-16) when compared to quartz sampled distal to the deposit (quartz KS-17). The Al concentrations in both samples are similar and relatively high. Both quartz lenses are characterized by $LREE_n$ enriched lanthanide distribution patterns with positive Ce anomalies (Fig. 5). In contrast to the two samples collected from outside the deposit, the three quartz samples (samples KS-4, KS-5, and KS-6) from the Nadeje adit show unstable yellowish green or blue CL colors that change to a stable brown CL during electron irradiation. The samples have relatively high Al and Sr concentrations and show kinked REE distributions with distinct positive Eu anomalies. The quartz KS-4 sampled from a gold-bearing vein (Au content of 22 ppm, Pertold, personal communication) exhibits the most intense Eu anomaly. Positive Ce anomalies were observed in two of the three samples (Fig. 5).

The quartz nodule collected from altered wall rocks in the Muruntau deposit (sample MT-6) and the hydrothermal vein quartz (samples MT-5 and MT-7) show stable bluish-black CL emissions. The samples from Muruntau have relatively low Al, Mg, and U contents. The lanthanide distribution patterns of quartz from Muruntau are $LREE_n$ enriched. A positive Ce anomaly is only present in the quartz nodule and a positive Eu anomaly was observed in the quartz sample located close to the 'Southern Fault' (Fig. 6). The hydrothermal quartz from Myutenbai (samples MT-1 and MT-3) is typified by a stable bluish-black CL. The REE distribution patterns of the two samples are $LREE_n$ enriched and display pronounced positive Eu anomalies (Fig. 6). The two samples are characterized by relatively high Al concentrations. They have elevated Mg and U concentrations when compared to the samples from Muruntau whereas the Sr contents are similar to those in samples from Muruntau.

5. Discussion

The present study demonstrates that metamorphic quartz bodies located distal to ore deposits are characterized by uniform and very low trace element concentrations despite variations in the metamorphic grade and wall rock compositions. The uniform composition of the metamorphic quartz samples can be explained by recrystallization of the quartz. Recrystallization occurred in

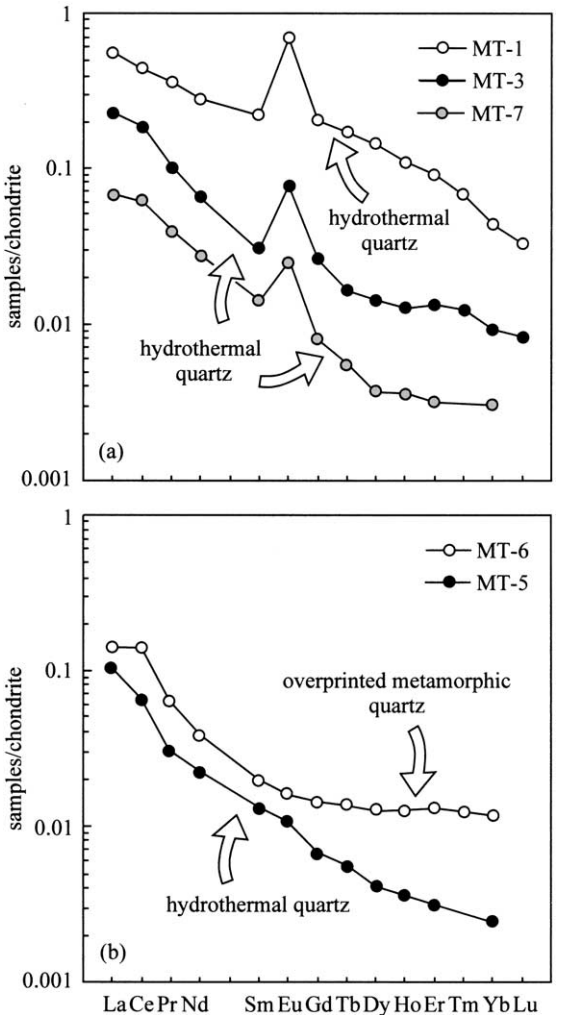

Fig. 6. Chondrite normalized lanthanide distributions of quartz from the Muruntau and Myutenbai gold deposits, Uzbekistan: (a) REE distribution patterns of samples MT-1 and MT-3 from Myutenbai as well as of quartz MT-7 from Muruntau and (b) REE distribution patterns of samples MT-5 and MT-6 from Muruntau.

response to strain as suggested by the microtextures and the brownish and yellow CL colors characteristic for recrystallized quartz from regional metamorphic rocks [26]. In particular, recovery phenomena may have played a key role in the release of strain from the quartz crystals and are also likely to have caused a purification of the quartz. However, the composition of the precursor material is possibly recorded in the variable Ce anomalies because it is conspicuous that positive Ce anomalies occur in most metamorphic quartz samples hosted by mica schist or paragneiss.

Quartz samples located within the alteration halo of tin deposits show trace element signatures that deviate significantly from the unaltered equivalents sampled distal to mineralization. These differences are interpreted to result from the interaction of the pre-existing quartz with the hydrothermal fluids. Hydrothermal alteration of pre-existing quartz may also explain the unstable green or blue CL colors of quartz sampled proximal to mineralization because this CL behavior was not observed in the unaltered equivalents. In contrast to the CL microscopy, the study of the quartz microtextures provides little evidence to identify alteration processes because the hydrothermal overprint of the pre-existing quartz was typically not associated with the precipitation of secondary quartz or recrystallization. However, the formation of trails of secondary fluid inclusions observed in some samples may have been related to the hydrothermal alteration of the quartz.

The differences between the trace element signatures of altered quartz and quartz collected from outside the alteration halos can be used to constrain the chemical environment of alteration of the quartz. In the case of the tin deposits in the Middle Erzgebirge, the hydrothermally altered samples have significantly higher Li, K, and Y contents than unaltered equivalents suggesting that these elements were added to the pre-existing quartz from the hydrothermal fluids. Moreover, the hydrothermal fluids must have been relatively enriched in Rb (Fig. 7). These findings are in good agreement with the results of previous geochemical and mineralogical studies suggesting that

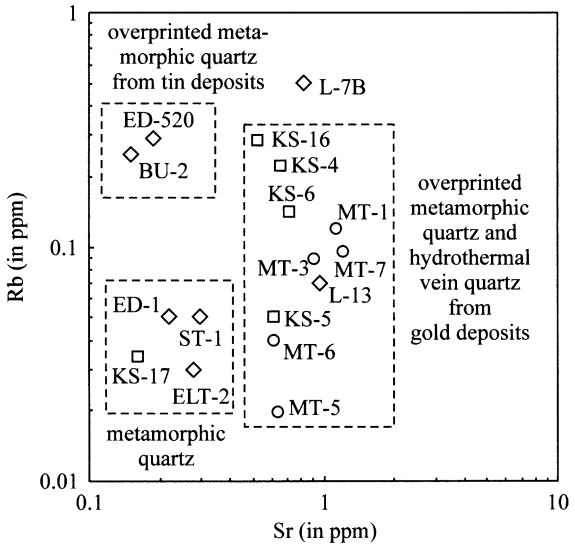

Fig. 7. Diagram of Rb versus Sr for all investigated quartz samples. The analyzed metamorphic quartz samples can be readily distinguished from hydrothermally altered metamorphic quartz as well as hydrothermal vein quartz from the investigated tin and gold deposits.

Li, Rb, and K were extremely enriched in the tin deposit-forming hydrothermal–magmatic system [15,16,27]. Another conspicuous feature of the metamorphic quartz samples collected close to the tin mineralization in the Middle Erzgebirge is the elevated Al content. Elevated concentrations of this element in the samples can be readily explained by the hydrothermal alteration because the incorporation of Al on the Si site of the quartz crystal structure increases with temperature [28].

The variations in the lanthanide distribution patterns of the quartz samples from the Middle Erzgebirge provide additional constraints on the nature of the mineralizing hydrothermal fluids. Unaltered metamorphic quartz is characterized by $LREE_n$ enriched lanthanide distribution patterns with variable positive Ce anomalies. In contrast, hydrothermally altered quartz contained in metamorphic rocks close to the granite (28 m to the granite contact) shows a relative enrichment of the $HREE_n$, a positive Eu anomaly, and a smaller Ce anomaly. However, at an increased distance to the granite ($\sim$300 m to the granite contact), altered metamorphic quartz displays

REE distribution patterns superficially resembling that of unaltered metamorphic quartz. Assuming that metamorphic quartz samples collected at different distances to the granite were characterized by similar REE distribution patterns prior to the deposit formation (with the exception of possible variations in the Ce anomalies), it has to be concluded that quartz close to the granite was overprinted by hydrothermal fluids showing a $HREE_n$ enrichment and a positive Eu anomaly whereas quartz located at a larger distance interacted with a $LREE_n$ enriched hydrothermal fluid lacking a positive Eu anomaly. This suggests that the REE distribution pattern of the hydrothermal fluids changed during fluid migration.

The chemical evolution of the hydrothermal fluids in the exocontact of the Ehrenfriedersdorf deposit reconstructed from the quartz REE data is consistent with the results of similar studies on fluorite samples from the Ehrenfriedersdorf deposit [29,30] and other tin deposits in the Erzgebirge district [31,32] suggesting that the REE content of hydrothermally altered quartz mirrors the composition of the hydrothermal fluids. The REE patterns of early endocontact fluorite samples were found to exhibit a pronounced $HREE_n$ enrichment whereas the lanthanide distributions of exocontact fluorite samples resulted from mixing of this $HREE_n$ enriched fluid with a component derived from the $LREE_n$ enriched wall rocks. Late stage fluorite samples were found to be characterized by $LREE_n$ enriched distribution patterns. The interaction of the $HREE_n$ enriched fluids with the granitic melt at high temperatures and reducing conditions resulted in an Eu depletion in the granite (strong negative Eu anomaly) and in an Eu enrichment in the hydrothermal fluids (positive Eu anomaly). This process resulted in the observed positive Eu anomalies in REE distribution patterns of quartz and fluorite from the exocontact [31].

Comparison of the CL properties and chemical signatures of quartz samples collected in the Middle Erzgebirge with the characteristics of the two samples from Lauenstein indicates that the quartz body from Lauenstein cannot be simply regarded as 'typically metamorphic' in origin as suggested by Heynke et al. [8]. The elevated contents of Li, K, Rb, and Al suggest that the first generation quartz represents a pre-existing metamorphic (?) quartz that was intensely overprinted by hydrothermal fluids. Moreover, the second generation quartz clearly formed as a result of a hydrothermal event affecting the vein-like quartz body at Lauenstein. Although the trace element data of the quartz samples may suggest that the hydrothermal fluids were similar in nature to the ore-forming fluids in the Middle Erzgebirge, the source of the hydrothermal fluids involved in the quartz formation and alteration at Lauenstein was not further constrained in the present study.

Metamorphic quartz samples collected at different distances to gold mineralization also have CL properties and chemical characteristics that are distinctly different from unaltered metamorphic equivalents. Quartz from the alteration halo of the gold mineralization at Kašperské Hory and the gold deposits Muruntau and Myutenbai typically shows stable bluish-black CL colors that are similar to those observed for the hydrothermal vein quartz from Muruntau and Myutenbai.

Hydrothermally altered quartz and hydrothermal vein quartz from the gold deposits is typified by relatively high Sr contents (Fig. 7). The hydrothermal vein quartz commonly displays positive Eu anomalies and elevated Al concentrations. These findings are in agreement with previous trace element studies on quartz from gold deposits [5,12,14]. The trace element contents of the quartz from the gold deposits can be used to derive information on the composition of the mineralizing hydrothermal fluids. In particular, comparison of the trace element signatures of quartz and associated scheelite may be useful to constrain the chemical attributes of the mineralizing fluids [33]. The enrichment of Sr in quartz and associated scheelite from Kašperské Hory, Muruntau, and Myutenbai indicates that the mineralizing hydrothermal fluids were typified by elevated concentrations of this element ([33] and unpublished data). Due to the fact that Sr isotope ratios of scheelite and quartz vein samples from Muruntau and Myutenbai are in equilibrium with the schist hosting the mineralization [22,34], it is inferred that the Sr enrichment in the fluids occurred during the interaction of the hydrothermal fluids with

the wall rocks due to plagioclase alteration [33]. Because there is no obvious correlation between the size of the Eu anomalies and the behavior of Sr, it is not clear whether the anomalous behavior of Eu may also be accounted for by alteration of feldspar contained in the wall rocks. In this context it is important to note that a granite body discovered by deep drilling below the Myutenbai deposit is strongly depleted in Eu and enriched in U (Kempe and Graupner, unpublished). Because quartz and scheelite samples from Myutenbai show positive Eu anomalies and U enrichments, it appears possible that fluids interacting with the granite below the Myutenbai deposit were involved in the ore-forming process.

6. Conclusions

The present reconnaissance study demonstrates that low level analysis of quartz by modern ICP-MS techniques yields accurate and precise trace element data that provide genetic information. The analysis of carefully selected samples from the tin mining district Erzgebirge, Germany, the gold-quartz vein deposit Kašperské Hory, Czech Republic, and the gold deposits of Muruntau and Myutenbai, Uzbekistan, clearly showed that metamorphic and hydrothermal quartz can be discriminated on the basis of their trace element signatures.

Metamorphic quartz was found to be characterized by low trace element concentrations when compared to hydrothermal vein quartz. In particular, the low concentrations of Li, Al, K, Rb, Sr, and Y represent useful indicators that can be used to discriminate between quartz recrystallized during metamorphism and quartz of hydrothermal origin. In addition to low concentrations of these indicator elements, metamorphic quartz was found to be typified by $LREE_n$ enriched lanthanide distribution patterns showing variable Ce anomalies whereas the REE distribution patterns of hydrothermal quartz are commonly $HREE_n$ enriched and may show positive Eu anomalies. The trace element signatures of quartz can also be used to identify hydrothermal alteration of pre-existing metamorphic quartz located within alteration halos enveloping hydrothermal tin and gold deposits. The present study also demonstrates that the trace element signatures of altered metamorphic quartz and hydrothermal vein quartz allow a discrimination between quartz associated with tin mineralization and quartz from gold deposits, especially when using their Rb and Sr contents. The trace element contents of quartz from ore deposits are interpreted to be primarily controlled by the composition of the quartz-forming hydrothermal fluids as evidenced by the similarity of the trace element characteristics of quartz and associated minerals such as fluorite and scheelite.

Based on the findings of the present investigation, it is concluded that the chemical composition of quartz is highly sensitive to secondary processes such as hydrothermal alteration and metamorphic recrystallization. Preliminary discrimination between quartz of different origin may be carried out by combining field evidence with CL microscopy. Subsequent trace element analysis of quartz yields additional information that allow a more detailed reconstruction of the chemical environment of quartz formation and alteration.

Acknowledgements

We express our gratitude to G. Bombach, P. Dulski, W. Klemm, M. Krebetschek, S. Tesch, and T. Trautmann for their analytical expertise. We thank A. Van den Kerkhof and an anonymous reviewer for critical comments improving the manuscript. This paper has benefited from discussions with P.M. Herzig, D. Wolf, and D. Leonhardt. Field work at Kašperské Hory, Muruntau, and Myutenbai was kindly supported by Z. Pertold, A.A. Kremenetsky, and A.D. Aksenov. The DAAD provided travel funds to Uzbekistan. T.M. acknowledges financial support by the German National Merit Foundation.*[AC]*

References

[1] H.U. Bambauer, Spurenelementgehalte und γ-Farbzentren

in Quarzen aus Zerrklüften der Schweizer Alpen, Schweiz, Mineral. Petrol. Mitt. 41 (1961) 335–369.
[2] L.J. Suttner, R.K. Leininger, Comparison of the trace element content of plutonic, volcanic, and metamorphic quartz from southwestern Montana, Geol. Soc. Am. Bull. 83 (1972) 1855–1862.
[3] J. Gerler, C. Schnier, Neutron activation analysis of liquid inclusions exemplified by a quartz sample from the Ramsbeck Mine, F.R.G., Nucl. Geophys. 3 (1989) 41–48.
[4] J. Götze, R. Lewis, Distribution of REE and trace elements in size and mineral fractions of high-purity quartz sands, Chem. Geol. 114 (1994) 43–57.
[5] J.C. van Moort, The chemical composition and paramagnetism of auriferous quartz, Mineral. Mag. 58A (1994) 625–626.
[6] G.R. Watt, P. Wright, S. Galloway, C. McLean, Cathodoluminescence and trace element zoning in quartz phenocrysts and xenocrysts, Geochim. Cosmochim. Acta 61 (1997) 4337–4348.
[7] K. Wünsch, Zur Mineralassoziation und Spurenelementgeochemie metamorphogener Quarzkörper im Südteil der DDR, Z. Angew. Geol. 36 (1990) 54–59.
[8] U. Heynke, O. Leeder, H. Schulz, On distinguishing quartz of hydrothermal or metamorphogenic origin in different monomineralic veins in the eastern part of Germany, Mineral. Petrol. 46 (1992) 315–329.
[9] C. Grappin, M. Treuil, S. Yaman, J.C. Touray, Le spèctre des terres rares de la fluorine en tant que marqueur des propriétés du milieu de dépôt et des interactions entre solutions minéralisantes et roches sources. Exemple pris dans le Destrict de la Marche Occidentale (France), Mineral. Deposita 14 (1979) 297–309.
[10] M. Bau, P. Möller, Rare earth element fractionation in metamorphogenic hydrothermal calcite, magnesite and siderite, Mineral. Petrol. 45 (1992) 231–246.
[11] L. Raimbault, A. Baumer, M. Dubru, C. Benkerrou, V. Croze, A. Zahm, REE fractionation between scheelite and apatite in hydrothermal conditions, Am. Mineral. 78 (1993) 1275–1285.
[12] M.I. Novgorodova, V.M. Veretennikov, R.V. Boyarskaya, V.I. Drynkin, Geochemistry of trace elements in gold-bearing quartz, Geochem. Int. 21 (1984) 101–113.
[13] B. Peucker-Ehrenbrink, C. Schnier, Investigation of rare earth elements in quartz from the Bavarian Pfahl, Germany, by means of instrumental neutron activation analysis, Nucl. Geophys. 6 (1992) 249–260.
[14] S.F. Vinokurov, V.A. Kovalenker, Y.G. Safonov, A.L. Kerzin, REE in quartz from epithermal gold deposits: distribution and genetic implications, Geochem. Int. 37 (1999) 145–152.
[15] G. Hösel, Das Zinnerz-Lagerstättengebiet Ehrenfriedersdorf/Erzgebirge, Landesamt für Umwelt und Geologie und Oberbergamt, Freiberg, 1994, 196 pp.
[16] G. Hösel, H. Meyer, R. Seltmann, U. Tägl, Tin-bearing deposits of the Ehrenfriedersdorf district, in: R. Seltmann, H. Kämpf, P. Möller (Eds.), Metallogeny of Collisional Orogens Focussed on the Erzgebirge and Comparable Metallogenic Settings, Czech Geological Survey, Prague, 1994, pp. 129–136.
[17] Z. Pertold, M. Puncochár, Kašperské Hory ore district. Gold deposits of the central and SW part of the Bohemian Massif. Excursion Guide, Czech Geological Survey, Prague, 1995, pp. 87–104.
[18] J. Pertoldová, J. Fiala, M. Pudilová, M. Puncochár, M. Scharmová, P. Sztacho, Au-W mineralization of the Kašperské Hory ore district, SW Bohemia, Czechoslovakia, in: Y.T. Maurice (Ed.), Proceedings of the Eighth Quadrennial IAGOD Symposium, Schweizerbart'sche Verlagsbuchhandlung, Stuttgart, 1993, pp. 627–636.
[19] J. Durišová, L. Strnad, Z. Pertold, M. Pudilová, M.C. Boiron, Gold-bearing quartz veins in a regional shear zone: Kašperské Hory gold deposit (Bohemian Massif), in: J. Pasava, B. Kríbek, K. Zák (Eds.), Mineral Deposits: From Their Origin to Their Environmental Impacts, Balkema, Rotterdam, 1995, pp. 109–112.
[20] Y.I. Uspenskiy, A.P. Aleshin, Patterns of scheelite mineralization in the Muruntau gold deposit, Uzbekistan, Int. Geol. Rev. 35 (1993) 1037–1051.
[21] L.J. Drew, B.R. Berger, N.K. Kurbanov, Geology and structural evolution of the Muruntau gold deposit, Kyzylkum desert, Uzbekistan, Ore Geol. Rev. 11 (1996) 175–196.
[22] U. Kempe, B.V. Belyatsky, R.S. Krymsky, A.A. Kremenetsky, P.A. Ivanov, Sm-Nd and Sr isotope systematics of scheelite from the giant Au(-W) deposit Muruntau (Uzbekistan): implications for the age and sources of Au mineralization, Mineral. Deposita 36 (2001) 379–392.
[23] R.D. Neuser, A new high-intensity cathodoluminescence microscope and its application to weakly luminescing minerals, Bochumer Geol. Geotech. Arb. 44 (1995) 116–118.
[24] T. Monecke, G. Bombach, W. Klemm, U. Kempe, J. Götze, D. Wolf, Determination of trace elements in the quartz reference material UNS-SpS and in natural quartz samples by ICP-MS, Geostandards Newsl. 24 (2000) 73–81.
[25] E. Anders, N. Grevesse, Abundances of the elements: meteoritic and solar, Geochim. Cosmochim. Acta 53 (1989) 197–214.
[26] J. Götze, M. Plötze, D. Habermann, Origin, spectral characteristics and practical applications of the cathodoluminescence (CL) of quartz – a review, Mineral. Petrol. 71 (2001) 225–250.
[27] H. Gerstenberger, Autometasomatic Rb enrichments in highly evolved granites causing lowered Rb-Sr isochron intercepts, Earth Planet. Sci. Lett. 93 (1989) 65–75.
[28] W.H. Dennen, W.H. Blackburn, A. Quesada, Aluminum in quartz as a geothermometer, Contrib. Mineral. Petrol. 27 (1970) 332–342.
[29] T. Seifert, U. Kempe, Sn-W-Lagerstätten und spätvariszische Magmatite des Erzgebirges, Eur. J. Mineral. 6 (Beih. 2) (1994) 125–172.
[30] T. Monecke, J. Monecke, W. Mönch, U. Kempe, Mathematical analysis of rare earth element patterns of fluo-

rites from the Ehrenfriedersdorf tin deposit, Germany: evidence for a hydrothermal mixing process of lanthanides from two different sources, Mineral. Petrol. 70 (2000) 235–256.
[31] U. Kempe, S. Goldstein, Eu anomalies, tetrad effect and HREE enrichment in fluorites from Sn deposits: evidence for two source mixing and phase separation, J. Czech Geol. Soc. 42 (1997) 37.
[32] T. Monecke, U. Kempe, J. Monecke, M. Sala, D. Wolf, Tetrad effect in rare earth element distribution patterns: a method of quantification with application to rock and mineral samples from granite-related rare metal deposits, Geochim. Cosmochim. Acta 66 (2002) 1185–1196.
[33] U. Kempe, T. Monecke, T. Oberthür, A.A. Kremenetsky, Trace elements in scheelite and quartz from the Muruntau/Myutenbai gold deposit, Uzbekistan: constraints on the nature of the ore-forming fluids, in: C.J. Stanley et al. (Eds.), Mineral Deposits: Processes to Processing, Balkema, Rotterdam, 1999, pp. 373–376.
[34] Y.A. Kostitsyn, Rb-Sr isotopic study of the Muruntau deposit magmatism, metamorphism, and mineralization, Geokhimiya 12 (1996) 1123–1138.